Data-driven pole determination of (overlapping) resonances

(based on Phys. Lett. B 839, 137809 (2023))

Daniele Binosi[1], Alessandro Pilloni[2], **Ralf-Arno Tripolt**[3,4]

[1]ECT*, Trento
[2]University of Messina
[3]University of Giessen, [4]Helmholtz Research Academy Hesse for FAIR (HFHF)

"Accessing and Understanding the QCD Spectra", INT, Seattle, March 21, 2023

Outline

I) The Schlessinger Point Method (SPM)

- definition and simple examples
- analytic continuation to the complex plane

II) Application to experimental data

- setting up a suitable SPM algorithm
- benchmark on models for S-wave $J/\psi \to \gamma\pi^0\pi^0$ data
- application to BESIII data

III) Summary and outlook

Part I

The Schlessinger Point Method (SPM)

Schlessinger Point Method (SPM)

Given a finite set of N data points (x_i, y_i) we construct the rational interpolant $p(x)/q(x)$ with polynomials $p(x)$ and $q(x)$ that is given by the continued fraction

$$p(x)/q(x) = C_N(x) = \cfrac{y_1}{1 + \cfrac{a_1(x - x_1)}{1 + \cfrac{a_2(x - x_2)}{\vdots\, a_{N-1}(x - x_{N-1})}}}$$

where the coefficients a_i are given recursively by $a_1 = \frac{y_1/y_2 - 1}{x_2 - x_1}$ and

$$a_i = \frac{1}{x_i - x_{i+1}} \left(1 + \frac{a_{i-1}(x_{i+1} - x_{i-1})}{1+} \frac{a_{i-2}(x_{i+1} - x_{i-2})}{1+} \cdots \frac{a_1(x_{i+1} - x_1)}{1 - y_1/y_{i+1}} \right)$$

The polynomials $(p(x), q(x))$ are of order $(N/2 - 1, N/2)$ for an even number of input points and of order $((N-1)/2, (N-1)/2)$ for an odd number of input points

[L. Schlessinger, Physical Review, Volume 167, Number 5 (1968)]
[R.W. Haymaker and L. Schlessinger, Mathematics in Science and Engineering, Volume 71, Chapter 11 (1970)]
[H.J. Vidberg and J.W. Serene, Journal of Low Temperature Physics, Vol. 29, Nos. 3/4 (1977)]

Analytic continuation and regime of applicability

- an analytic continuation into the complex plane can be performed by choosing x in $C_N(x)$ to be complex, i.e. $x = \alpha e^{i\theta}$
- rational interpolants can exactly reproduce polar singularities, thus extending the 'radius of convergence' to the first non-polar singularity, e.g. a branch point (BP)
- even a branch cut may be well approximated by a series of poles of the rational fraction
- a rational fraction can have only one sheet in the complex plane - a many-sheeted function can only be reconstructed on a single sheet

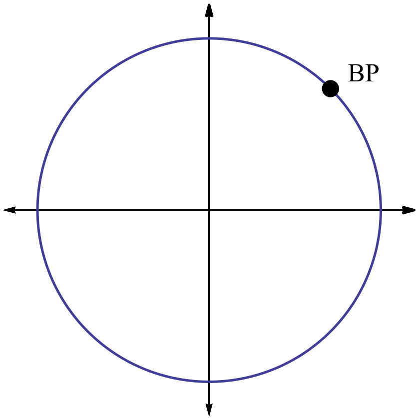

[R. de Montessus de Ballore, Bull. Soc. Math. France 30, 28 (1902)]
[P. Masjuan, J.J. Sanz-Cillero, Eur. Phys. J. C73, 2594 (2013)]
[R.-A. T., I. Haritan, J. Wambach, N. Moiseyev, Phys. Lett. B 774, 411-416 (2017)]
[R.-A. T., P. Gubler, M. Ulybyshev, L. v. Smekal, Comput. Phys. Commun. 237, 129-142 (2019)]
[D. Binosi, R.-A. T., Phys. Lett. B 801, 135171 (2020)]

Simple example: $f(x) = x$

For $N = 2$ input points:

- since N is even, the resulting rational interpolant will be of order $(N/2 - 1, N/2)$
- for $N = 2$ we expect

$$C_N(x) = \frac{p(x)}{q(x)} = \frac{p_0}{q_0 + q_1\, x}$$

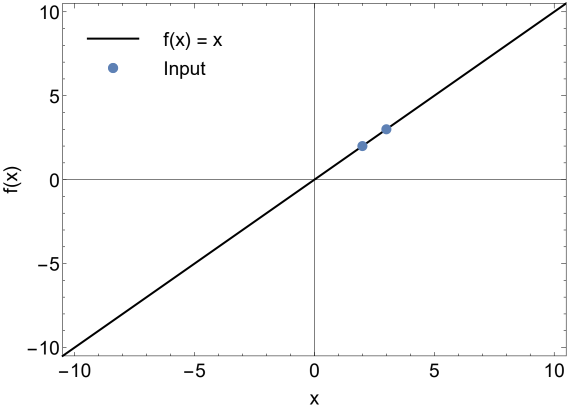

Simple example: $f(x) = x$

For $N = 2$ input points:

- since N is even, the resulting rational interpolant will be of order $(N/2 - 1, N/2)$
- for $N = 2$ we expect

$$C_N(x) = \frac{p(x)}{q(x)} = \frac{p_0}{q_0 + q_1\, x}$$

- the resulting SPM interpolator is given by

$$C_N(x) = \frac{1.2}{1 - 0.2\, x}$$

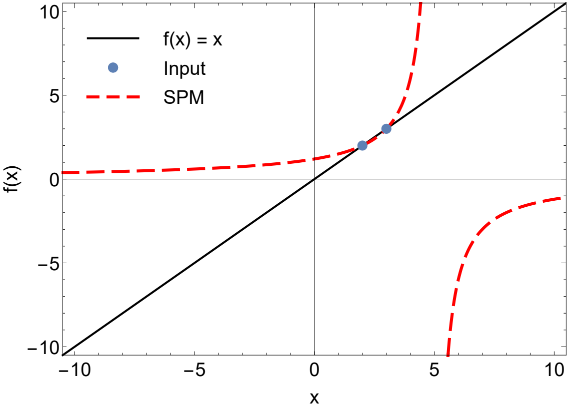

Simple example: $f(x) = x$

For $N = 3$ input points:

- since N is odd, the resulting rational interpolant will be of order $(N/2, N/2)$
- for $N = 3$ we expect

$$C_N(x) = \frac{p(x)}{q(x)} = \frac{p_0 + p_1\, x}{q_0 + q_1\, x}$$

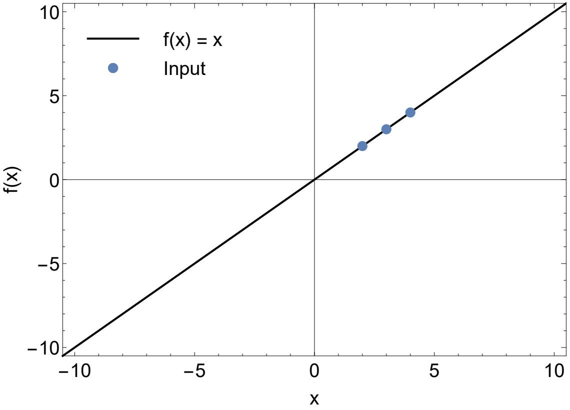

Simple example: $f(x) = x$

For $N = 3$ input points:

- since N is odd, the resulting rational interpolant will be of order $(N/2, N/2)$
- for $N = 3$ we expect

$$C_N(x) = \frac{p(x)}{q(x)} = \frac{p_0 + p_1\, x}{q_0 + q_1\, x}$$

- for exact data, the linear function is recovered, i.e. $\sim x/1$
- if we add noise of the order of $\mathcal{O}(10^{-15})$ we get, e.g.,

$$C_N(x) = \frac{1.81 \cdot 10^{-14} + x}{1 - 1.78 \cdot 10^{-15}\, x} \approx x$$

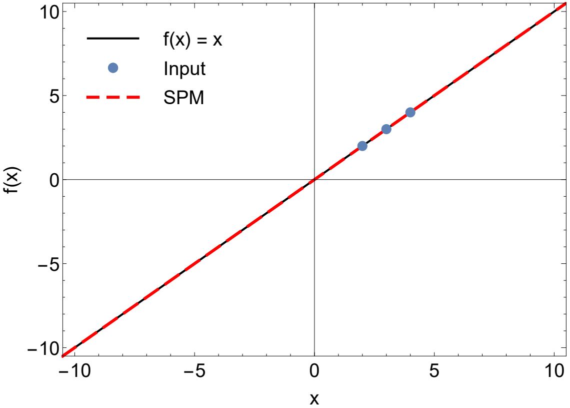

Simple example: $f(x) = x$

For $N = 4$ input points:

- since N is even, the resulting rational interpolant will be of order $(N/2 - 1, N/2)$
- for $N = 4$ we expect

$$C_N(x) = \frac{p(x)}{q(x)} = \frac{p_0 + p_1\, x}{q_0 + q_1\, x + q_2\, x^2}$$

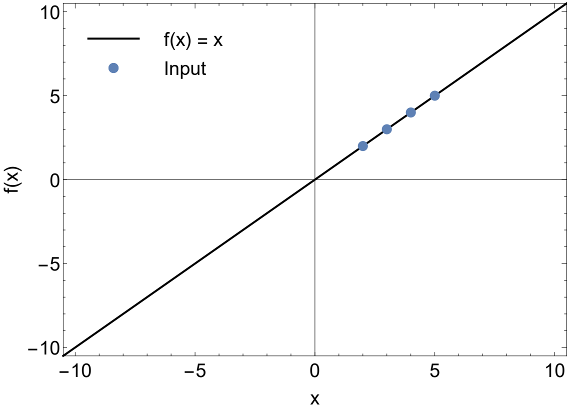

Simple example: $f(x) = x$

For $N = 4$ input points:

- since N is even, the resulting rational interpolant will be of order $(N/2 - 1, N/2)$
- for $N = 4$ we expect

$$C_N(x) = \frac{p(x)}{q(x)} = \frac{p_0 + p_1\, x}{q_0 + q_1\, x + q_2\, x^2}$$

- however, for exact data, the linear function is recovered, i.e. $\sim x/1$
- if we add noise of the order of $\mathcal{O}(10^{-15})$ we get, e.g.,

$$C_N(x) = \frac{-3.2 \cdot 10^{-14} + x}{1 + 1.2 \cdot 10^{-14}\, x - 1.3 \cdot 10^{-15}\, x^2}$$

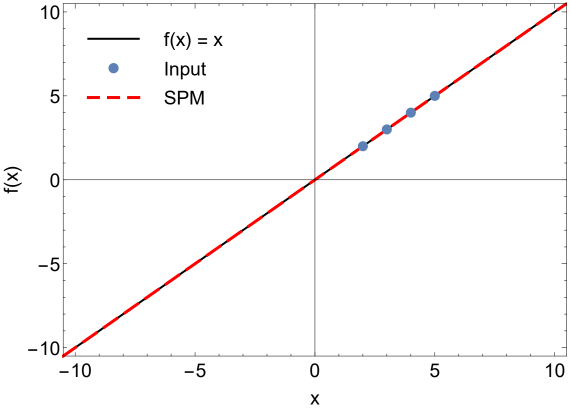

Breit-Wigner function

We use a Breit-Wigner function of the form

$$f(x) = \frac{A}{(x^2 - M^2)^2 + \gamma^2 M^2}$$

with parameters $A = 100$, $M = 4$, $\gamma = 2$

For $N = 14$ input points we expect

$$C_N(x) = \frac{p(x)}{q(x)} \sim \frac{\mathcal{O}(x^6)}{\mathcal{O}(x^7)}$$

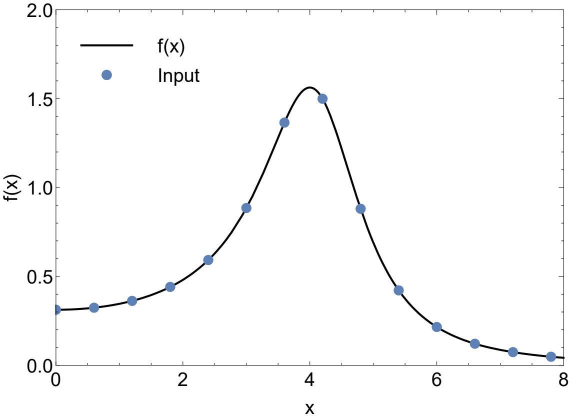

Breit-Wigner function

We use a Breit-Wigner function of the form

$$f(x) = \frac{A}{(x^2 - M^2)^2 + \gamma^2 M^2}$$

with parameters $A = 100,\ M = 4,\ \gamma = 2$

For $N = 14$ input points we expect

$$C_N(x) = \frac{p(x)}{q(x)} \sim \frac{\mathcal{O}(x^6)}{\mathcal{O}(x^7)}$$

with noise of the order of $\mathcal{O}(10^{-15})$ we get, e.g.,

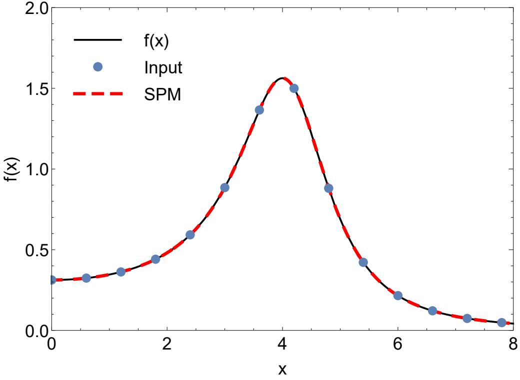

$$C_N(x) \approx \frac{0.313 - 0.2\,x + 0.04\,x^2 - 0.003\,x^3 - 10^{-14}\,x^4 + 10^{-16}\,x^5 + 10^{-17}\,x^6}{1 - 0.7\,x + 0.04\,x^2 + 0.06\,x^3 - 0.01\,x^4 - 0.001\,x^5 + 0.0004\,x^6 - 0.00002\,x^7}$$

$\rightarrow$ artificial poles (e.g. at $x \approx 2.3$) in denominator cancel with zeros in numerator!

Breit-Wigner function

Towards analytic continuation:

- evaluate SPM interpolation function $C_N(x)$ outside the input range
- describes Breit-Wigner function well for precise data!

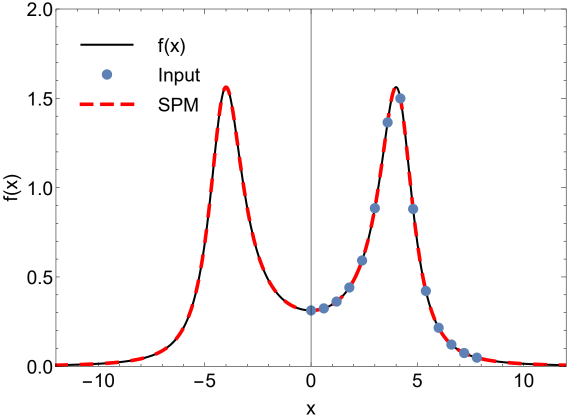

Breit-Wigner function

Analytic continuation:

- evaluate SPM interpolation function $C_N(x)$ for complex arguments: $x \to x + iy$
- describes Breit-Wigner function well for precise data!

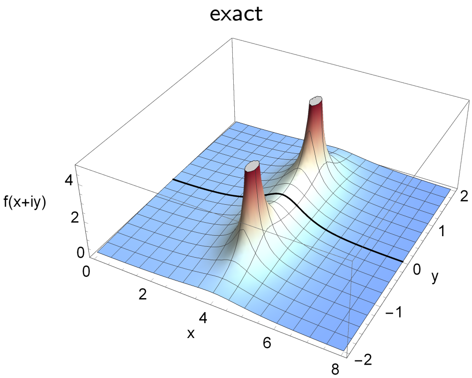

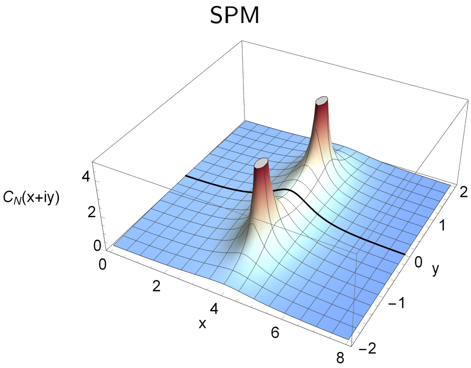

Breit-Wigner function with noise

We now add noise of $\mathcal{O}(10^{-1})$ to the same Breit-Wigner function of the form

$$f(x) = \frac{A}{(x^2 - M^2)^2 + \gamma^2 M^2}$$

with parameters $A = 100$, $M = 4$, $\gamma = 2$

For $N = 14$ input points we expect

$$C_N(x) = \frac{p(x)}{q(x)} \sim \frac{\mathcal{O}(x^6)}{\mathcal{O}(x^7)}$$

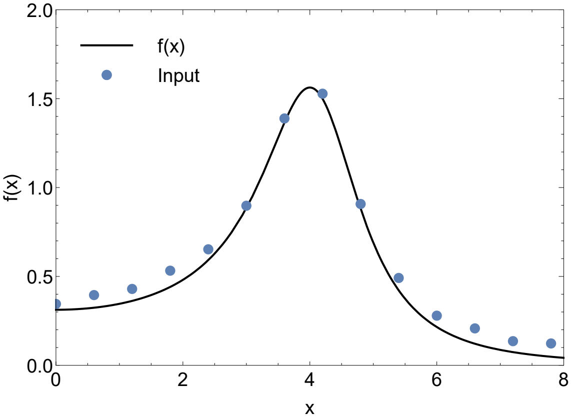

Breit-Wigner function with noise

We now add noise of $\mathcal{O}(10^{-1})$ to the same Breit-Wigner function of the form

$$f(x) = \frac{A}{(x^2 - M^2)^2 + \gamma^2 M^2}$$

with parameters $A = 100$, $M = 4$, $\gamma = 2$

For $N = 14$ input points we expect

$$C_N(x) = \frac{p(x)}{q(x)} \sim \frac{\mathcal{O}(x^6)}{\mathcal{O}(x^7)}$$

and get, e.g.,

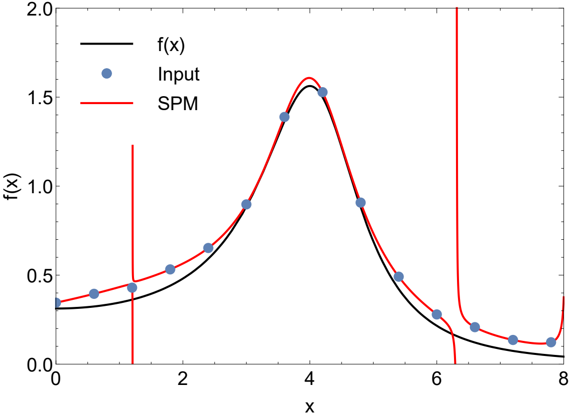

$$C_N(x) \approx \frac{0.345 - 0.6\,x + 0.3\,x^2 - 0.1\,x^3 + 0.01\,x^4 - 0.001\,x^5 + 0.00003\,x^6}{1 - 1.9\,x + 1.3\,x^2 - 0.5\,x^3 + 0.1\,x^4 - 0.02\,x^5 + 0.001\,x^6 - 0.00005\,x^7}$$

$\rightarrow$ artificial poles in denominator no longer cancel perfectly, but they (often) have small residues!

Breit-Wigner function with noise

Analytic continuation to the complex plane:

- main "particle" poles are slightly shifted by the noise but still clearly visible
- artificial poles can be identified due to their small residues and their random location (due to noise)

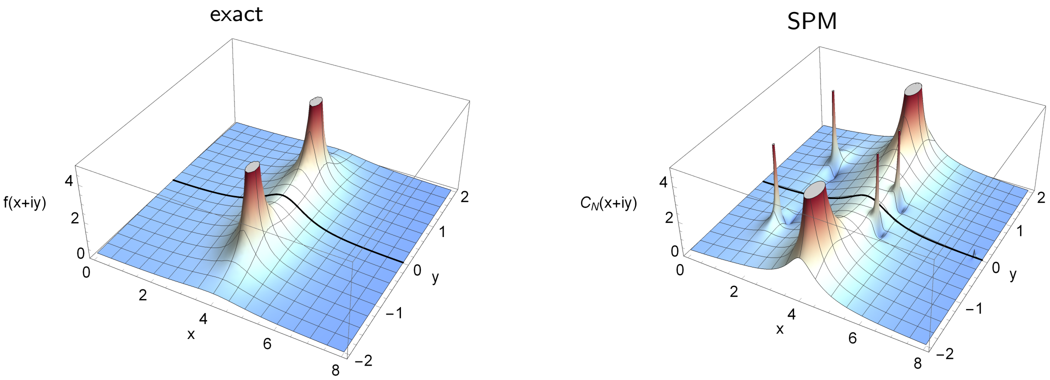

Part II

Application to experimental data

S-wave $J/\psi \to \gamma\pi^0\pi^0$ data from BESIII

- results show three peaks above 1 GeV, likely associated with $f_0(1500)$, $f_0(1710)$ and $f_0(2020)$
- together with the $f_0(1370)$ they are the main candidates for the lightest glueball
- process contributing to $J/\psi \to \gamma\pi^0\pi^0$:

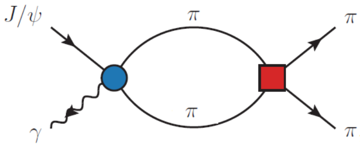

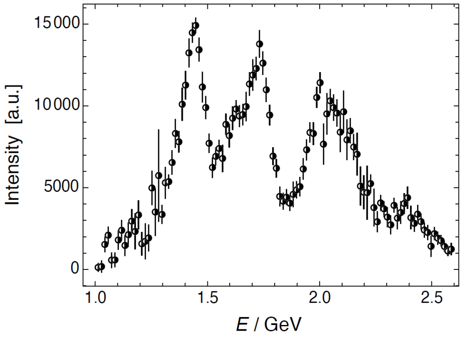

intensities for the 0^{++} amplitudes as a function of $M(\pi_0\pi_0)$

[M. Ablikim et al. (BESIII Collaboration), Phys. Rev. D 92, 052003 (2016)]
[JPAC Collaboration: A. Rodas, A. Pilloni, M. Albaladejo, C. Fernandez-Ramirez, V. Mathieu, A. P. Szczepaniak, Eur.Phys.J.C 82, 80 (2022)]
[D. Binosi, A. Pilloni, R.-A. T., Phys. Lett. B 839, 137809 (2023)]

Models

S- and D-wave intensities and relative phase of $J/\psi \to \gamma\pi^0\pi^0$ and $\to \gamma K_S^0 K_S^0$ were parametrized by JPAC based on the coupled-channel N/D formalism (using unitarity and dispersion relations):

$$I_i^J(s) = \mathcal{N} p_i \left| a_i^J(s) \right|^2$$

$$a_i^J(s) = E_\gamma\, p_i^J \sum_k n_k^J(s) \left[D^J(s)^{-1} \right]_{ki}$$

$$p_i = \sqrt{s - 4m_i^2}/2 \qquad E_\gamma = (m_{J/\psi}^2 - s)/(2\sqrt{s})$$

with $i = \pi\pi$ or $K\bar{K}$ and the invariant mass squared s.

The resulting **5 models (A-E)** contain either 3 or 4 poles and sometimes an additional branch point at $E = 1.52$ GeV from the stable $\rho\rho$ channel.

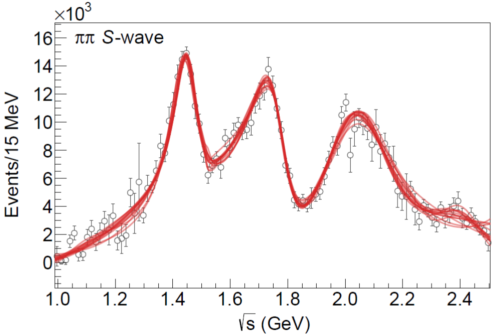

[JPAC Collaboration: A. Rodas, A. Pilloni, M. Albaladejo, C. Fernandez-Ramirez, V. Mathieu, A. P. Szczepaniak, Eur.Phys.J.C 82 (2022) 1, 80]
[D. Binosi, A. Pilloni, R.-A. T., Phys. Lett. B 839, 137809 (2023)]
[J.R. Pelaez, Physics Reports 658 (2016) 1]

Statistical SPM

data from model A

points with random errors

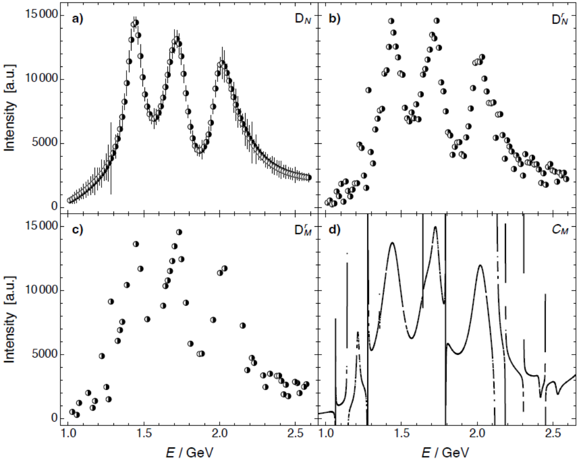

selecting 50 points randomly

SPM interpolation

SPM poles

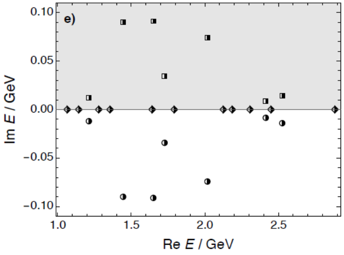

[D. Binosi, A. Pilloni, R.-A. T., Phys. Lett. B 839, 137809 (2023)]

Separating signal from noise

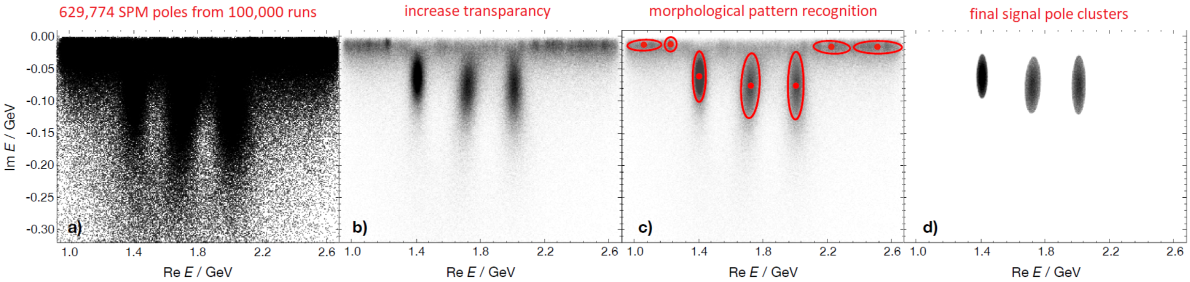

- on average, the number of signal poles is $\sim 20\%$ of all poles
- final signal pole clusters contain e.g. 50,000 poles which can be used to compute the standard deviation
- signal cluster are 'vertical', noise clusters (mostly) 'horizontal' and close to real axis
- we use the Mathematica commands: ColorNegate, MorphologicalBinarize and MorphologicalComponent

[D. Binosi, A. Pilloni, R.-A. T., Phys. Lett. B 839, 137809 (2023)]

Validation of the method - Model A - exact data

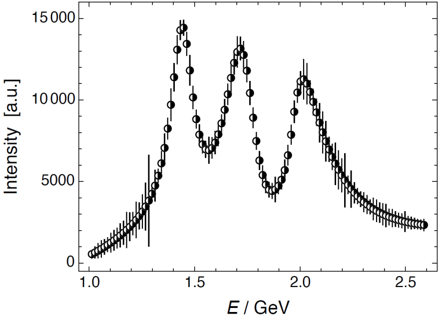

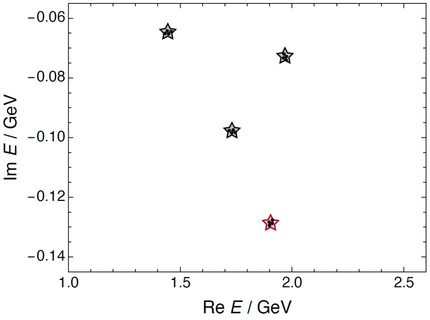

- all signal poles are correctly identified for exact data (i.e. data without uncertainties)!
- noise poles are almost exactly canceled by corresponding zeros in numerator

[D. Binosi, A. Pilloni, R.-A. T., Phys. Lett. B 839, 137809 (2023)]

Validation of the method - Model A

Model A

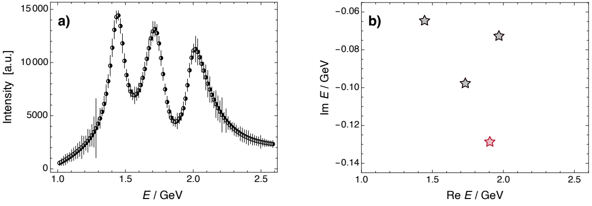

	1[st] pole (GeV)	2[nd] pole (GeV)	3[rd] pole (GeV)
Exact	1.44426 - i 0.06460	1.73160 - i 0.09773	1.96864 - i 0.07271
10% exp. error	1.4464(68) - i 0.066(7)	1.731(11) - i 0.092(11)	1.986(16) - i 0.088(20)
33% exp. error	1.447(11) - i 0.067(12)	1.728(17) - i 0.089(17)	1.984(14) - i 0.089(20)
Full exp. error	1.444(16) - i 0.063(17)	1.728(21) - i 0.073(19)	1.988(20) - i 0.074(22)

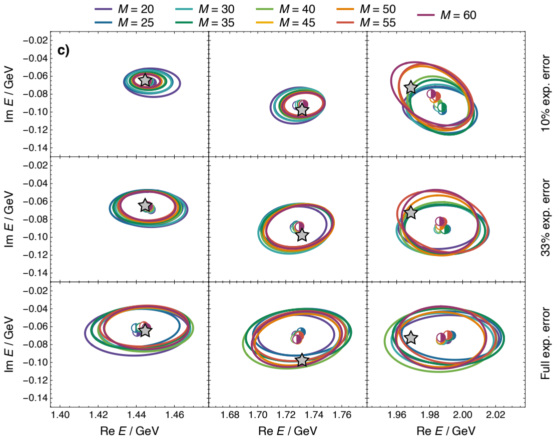

- different colors for ellipses correspond to different numbers of input points ($M = 20, \dots, 60$)
- 3 rows correspond to different amount of full experimental errors: 10%, 33%, 100%
- ellipses indicate 1σ (i.e. 68%) confidence regions

[D. Binosi, A. Pilloni, R.-A. T., Phys. Lett. B 839, 137809 (2023)]

Validation of the method - Model B

Model B

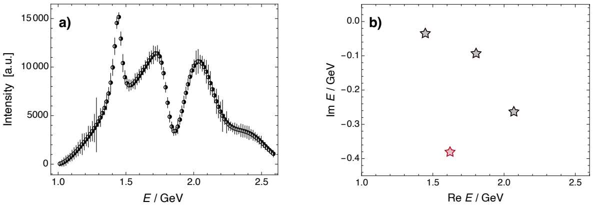

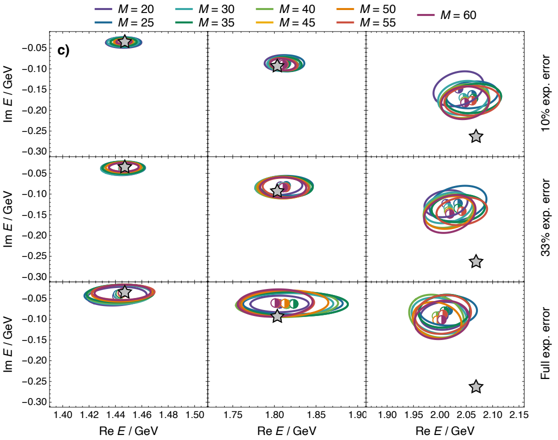

	1[st] pole (GeV)	2[nd] pole (GeV)	3[rd] pole (GeV)
Exact	1.44708 - *i* 0.03478	1.80350 - *i* 0.09319	2.06863 - *i* 0.26320
10% exp. error	1.4461(64) - *i* 0.0351(62)	1.811(12) - *i* 0.088(11)	2.044(31) - *i* 0.172(27)
33% exp. error	1.4459(97) - *i* 0.0366(95)	1.810(20) - *i* 0.083(17)	2.016(31) - *i* 0.138(27)
Full exp. error	1.444(16) - *i* 0.039(15)	1.810(34) - *i* 0.063(19)	2.000(33) - *i* 0.096(30)

- different colors for ellipses correspond to different numbers of input points $(M = 20, \ldots, 60)$
- 3 rows correspond to different amount of full experimental errors: 10%, 33%, 100%
- ellipses indicate 1σ (i.e. 68%) confidence regions

[D. Binosi, A. Pilloni, R.-A. T., Phys. Lett. B 839, 137809 (2023)]

Validation of the method - Model C

Model C

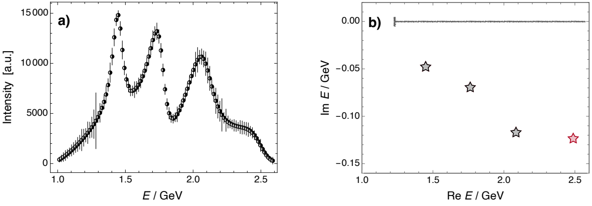

	1st pole (GeV)	2nd pole (GeV)	3rd pole (GeV)
Exact	1.44876 - i 0.04783	1.76273 - i 0.06952	2.08506 - i 0.11710
10% exp. error	1.4490(68) - i 0.0488(69)	1.7625(80) - i 0.0676(75)	2.076(17) - i 0.120(18)
33% exp. error	1.448(12) - i 0.052(13)	1.761(16) - i 0.067(15)	2.065(29) - i 0.113(30)
Full exp. error	1.445(17) - i 0.051(17)	1.759(21) - i 0.059(17)	2.050(30) - i 0.085(29)

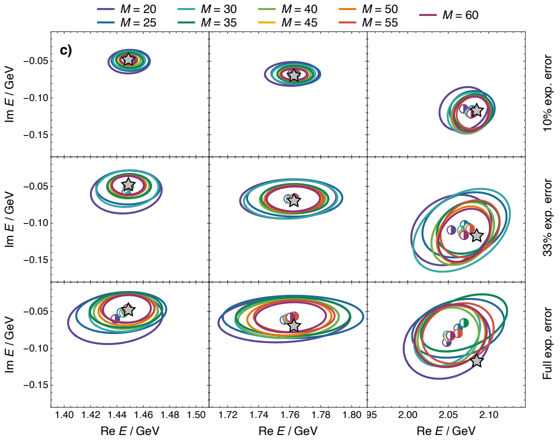

- different colors for ellipses correspond to different numbers of input points ($M = 20, \ldots, 60$)
- 3 rows correspond to different amount of full experimental errors: 10%, 33%, 100%
- ellipses indicate 1σ (i.e. 68%) confidence regions

[D. Binosi, A. Pilloni, R.-A. T., Phys. Lett. B 839, 137809 (2023)]

Validation of the method - Model D

Model D

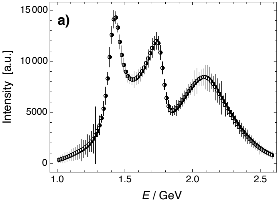

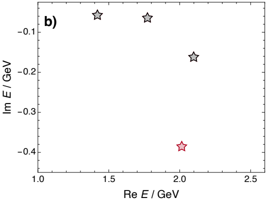

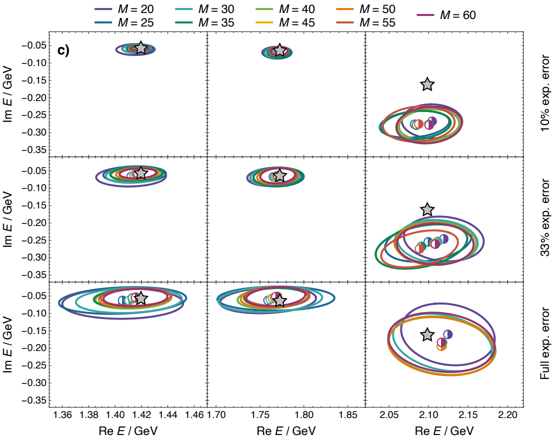

	1st pole (GeV)	2nd pole (GeV)	3rd pole (GeV)
Exact	1.41966 - *i* 0.05744	1.77254 - *i* 0.06434	2.09844 - *i* 0.16212
10% exp. error	1.4172(65) - *i* 0.0586(67)	1.7704(84) - *i* 0.0676(93)	2.101(27) - *i* 0.276(33)
33% exp. error	1.415(13) - *i* 0.061(14)	1.768(17) - *i* 0.066(17)	2.111(34) - *i* 0.255(41)
Full exp. error	1.412(23) - *i* 0.061(22)	1.764(30) - *i* 0.057(22)	2.118(44) - *i* 0.183(56)

- different colors for ellipses correspond to different numbers of input points $(M = 20, \ldots, 60)$
- 3 rows correspond to different amount of full experimental errors: 10%, 33%, 100%
- ellipses indicate 1σ (i.e. 68%) confidence regions

[D. Binosi, A. Pilloni, R.-A. T., Phys. Lett. B 839, 137809 (2023)]

Validation of the method - Model E

Model E

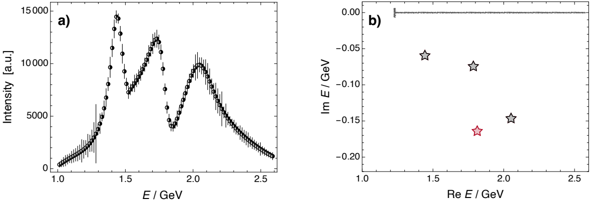

	1st pole (GeV)	2nd pole (GeV)	3rd pole (GeV)
Exact	1.44318 - *i* 0.05946	1.78532 - *i* 0.07444	2.05166 - *i* 0.14648
10% exp. error	1.450(27) - *i* 0.055(13)	1.783(10) - *i* 0.073(10)	2.022(28) - *i* 0.172(43)
33% exp. error	1.444(23) - *i* 0.054(14)	1.782(16) - *i* 0.073(15)	2.012(26) - *i* 0.188(37)
Full exp. error	1.438(27) - *i* 0.054(19)	1.779(28) - *i* 0.062(21)	2.020(37) - *i* 0.136(41)

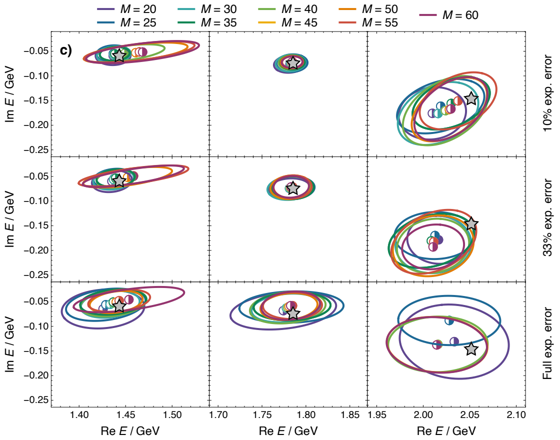

- different colors for ellipses correspond to different numbers of input points ($M = 20, \ldots, 60$)
- 3 rows correspond to different amount of full experimental errors: 10%, 33%, 100%
- ellipses indicate 1σ (i.e. 68%) confidence regions

[D. Binosi, A. Pilloni, R.-A. T., Phys. Lett. B 839, 137809 (2023)]

Application to BESIII data

Experimental data

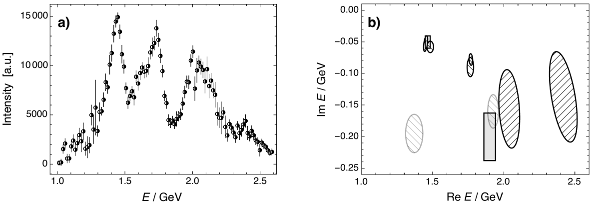

	1st pole (GeV)	2nd pole (GeV)	3rd pole (GeV)
Full exp. error	1.449(24) - *i* 0.050(17)	1.763(23) - *i* 0.052(17)	1.983(31) - *i* 0.071(27)

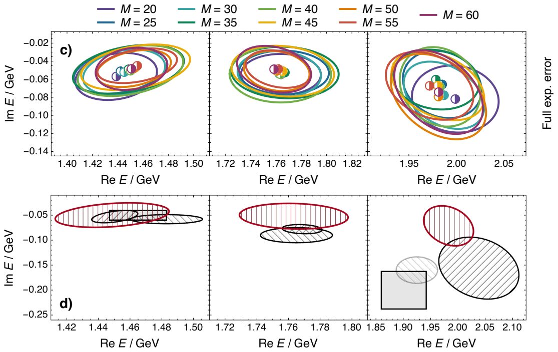

- extracted poles (likely associated with $f_0(1500)$, $f_0(1710)$ and $f_0(2020)$) in good agreement with literature

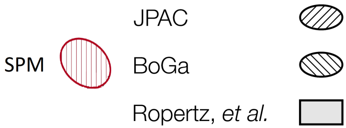

[D. Binosi, A. Pilloni, R.-A. T., Phys. Lett. B 839, 137809 (2023)]
[JPAC Collaboration: A. Rodas, A. Pilloni, M. Albaladejo, C. Fernandez-Ramirez, V. Mathieu, A. P. Szczepaniak, Eur.Phys.J.C 82, 80 (2022)]
[Bonn-Gatchina: A. V. Sarantsev, I. Denisenko, U. Thoma, E. Klempt, Phys. Lett. B816, 136227 (2021)]
[S. Ropertz, C. Hanhart, B. Kubis, Eur. Phys. J. C78, 1000 (2018)]

Application to BESIII data

Pole positions obtained from different data analyses (in MeV):

	SPM (this work)	JPAC	Bonn-Gatchina	Ropertz *et al.*
$f_0(1500)$	$(1449 \pm 24) - i(100 \pm 32)/2$	$(1450 \pm 10) - i(106 \pm 16)/2$	$(1483 \pm 15) - i(116 \pm 12)/2$	$(1465 \pm 18) - i(101 \pm 20)/2$
$f_0(1710)$	$(1763 \pm 23) - i(104 \pm 34)/2$	$(1769 \pm 8) - i(156 \pm 12)/2$	$(1765 \pm 15) - i(180 \pm 20)/2$	/
$f_0(2020)$	$(1983 \pm 31) - i(143 \pm 54)/2$	$(2038 \pm 48) - i(312 \pm 82)/2$	$(1925 \pm 25) - i(320 \pm 35)/2$ $(2075 \pm 20) - i(260 \pm 25)/2$	$(1901 \pm 41) - i(401 \pm 76)/2$

- extracted poles (likely associated with $f_0(1500)$, $f_0(1710)$ and $f_0(2020)$) in good agreement with literature
- other determinations include information from other channels, SPM only uses $J/\psi \to \gamma\pi^0\pi^0$ data!

[D. Binosi, A. Pilloni, R.-A. T., Phys. Lett. B 839, 137809 (2023)]
[JPAC Collaboration: A. Rodas, A. Pilloni, M. Albaladejo, C. Fernandez-Ramirez, V. Mathieu, A. P. Szczepaniak, Eur.Phys.J.C 82, 80 (2022)]
[Bonn-Gatchina: A. V. Sarantsev, I. Denisenko, U. Thoma, E. Klempt, Phys. Lett. B816, 136227 (2021)]
[S. Ropertz, C. Hanhart, B. Kubis, Eur. Phys. J. C78, 1000 (2018)]

Summary and Outlook

We presented a data-driven method for the determination of complex poles associated to resonances from experimental data:

- based on the Schlessinger Point Method (SPM) which interpolates a given data set by a continued-fraction expression
- analytic continuation to the complex plane allows to study pole structure
- SPM is able to compete with traditional (model dependent) analysis techniques, complementing them towards a robust determination of complex poles

Outlook:

- extension to coupled-channel datasets